Rheological Evidence for a Dynamical Crossover in Polymer Melts via Nonequilibrium Molecular Dynamics

Martin Kröger[1,2] and Siegfried Hess[1]

[1]*Institut für Theoretische Physik, Technische Universität Berlin, Hardenbergstrasse 36, D-10623 Berlin, Germany*
[2]*Polymer Physics, Institute of Polymers, ML H 18, ETH Zürich, CH–8092 Zürich, Switzerland*

(Received 16 December 1999)

A certain "critical" molecular weight controls rheological properties of the multibead finitely extensible nonlinear elastic (FENE) chain model polymer melt. The rheological crossover manifests itself in a change of power law behavior for the viscous properties at a critical number of beads per chain $N_c = 100 \pm 10$. This finding confirms a newly proposed relationship between dimensionless critical weight, characteristic length, and flexibility which we obtain as a side result. Results further suggest that the entanglement molecular weight N_e for the flexible FENE chain model could be comparable in size or even larger than its critical molecular weight N_c.

PACS numbers: 83.10.Nn, 83.50.Ax

A dense collection of repulsive linear chains made of mass points (beads) interconnected by finitely extensible nonlinear elastic (FENE) springs serves as a suitable coarse-grained model for polymer melts. The "multibead FENE model polymer" investigated in this study predicts many of the experimentally observed static and dynamic—in particular rheological—properties of polymer melts. At low and intermediate chain lengths, the nonlinear viscoelastic and structural properties such as viscosities and scattering patterns are in accordance with experimental results for shear and elongational flows [1–3]. Because of the computational demands caused by the strong increase of relaxation time with molecular weight (M) no proof had been presented so far that (or where) the basic multibead chain model also exhibits the experimentally observed rheological crossover. The crossover manifests itself in a change of power law for the zero shear viscosities at a certain M. For the particular system studied here the critical chain length is $N_c = 100 \pm 10$. A generalization of this result to polymer melts with arbitrary characteristics is given below.

"Topological" constraints hinder the motion of long polymers in melts and concentrated solutions [4]. This is well accepted since the works of Treloar 1940 on uncrosslinked rubbery polymers, of Bueche 1952 on entanglement networks, Edwards 1967 on knots formed by macromolecules, de Gennes 1971 on "reptation," and Doi and Edwards 1978 on the "tube model." Experimental evidence for topological constraints is rich, cf. [5]. In view of experimental results on relatively stiff molecules [6]the coupling should involve looping of chains around each other in their long-range contour [4]. There is ongoing discussion about a "microscopic" definition of "entanglement" [4,7,8]. Below, we report about scaling behaviors for the critical and entanglement M which help to interpret such a quantity.

Based on the measurement of single chain diffusion coefficients for the FENE model polymer melt obtained from equilibrium molecular dynamics (MD) simulations [9] with up to $N = 400$ beads per chain a "dynamical" crossover has been already observed. A characteristic length $N \approx 35$ was found which marks the crossover between "Rouse" to "reptation" diffusion regimes, for which the diffusion coefficients scale as $D \propto 1/N$ and $D \propto 1/N^2$, respectively. For the same model with 200 beads, Gao and Weiner [10] investigated the atomic mobility and found that intrachain beads of relatively low mobility tended to cluster in groups along the chain. Although the clustering introduces graininess in mobility and a possible new length scale their search for entanglements didn't lead to conclusive statements from equilibrium simulations. So far, up to April 2000, a characteristic slowdown of the diffusivity had been reported from simulations. The proof, that, and where a rheological crossover (at N_c) is present in the same flexible chain model was missing and will be given in this work. The plateau modulus G_N^0, from which the entanglement M_e can be rigorously deduced [11] has been reported for the FENE model in Ref. [12] for chains up to $N = 10^4$ (during revision of our manuscript) from the shear stress plateau during relaxation after step strain. The reported value is about a factor 2.3 larger than the one reported for the dynamical crossover above, and thus much closer to the one we are going to predict in this study.

The many-chain FENE model allows for a test of assumptions, in particular for the setup of single-chain theories, and motivates the required modifications such as end effects [13]. The original Doi-Edwards tube model [14] predicts unobserved flow instabilities and the nonexistence of over/undershoots in stress reversal experiments. It has been recently improved by considering "double reptation," "chain stretching," "constraint release," by avoiding the "independent alignment approximation" in order to describe features such as shear thinning, stress overshoots, recovery, Weissenberg effect as present in real and FENE polymer melts. The many-chain model does not rely on such assumptions. It offers insight into

 0031-9007/00/85(5)/1128(4)$15.00

the microscopic origin of nonlinear viscoelastic behavior of polymers.

In order to study the nonlinear viscoelastic properties of model polymer melts with various degrees of M we performed nonequilibrium MD (NEMD) simulations of FENE chains at constant bead number (bulk) density $n^* = 0.84$ in a cubic cell with periodic boundary conditions as described in [1]. The asterisk marks a quantity given in dimensionless Lennard-Jones (LJ) units. The repulsive part of the LJ potential is used to model excluded volume. For beads which are nearest neighbors along the chain, an attractive FENE potential: $U_{ij} = -0.5k^*R_0^{*2}\ln[1 - (r_{ij}^*/R_0^*)^2]$ (for $r_{ij}^* \le R_0^*$, otherwise $U_{ij} = \infty$) is added. The FENE spring $k^* = 30$ chosen is strong enough to make bond crossings energetically infeasible and small enough to choose a reasonable integration time step $\Delta t^* \approx 0.008$. With the choice for the finite extensibility of the FENE-spring $R_0^* = 1.5$ and its strength at constant temperature $T^* = 1$ we follow the works in [1,9]. All of the simulated systems presented here consist of 3×10^5 beads arranged in chains with $N = 4$–400 beads each. A stationary, planar Couette flow in x direction (gradient in y direction) with shear rate $\gamma = \partial v_x/\partial y$ was imposed [1]. Neighbor lists and layered link cells [15] are used to optimize the computer routines. In contrast to the standard procedure for equilibrium simulations, we update the list of pair dependencies on an upper limit for the increase of the relative separation of these pairs, not on the absolute motion of individual particles. Temperature was kept constant by rescaling the magnitude of the peculiar particle velocities which corresponds to the Gaussian constraint of constant kinetic energy.

The main contribution to the rheological properties for the dense system stems from the potential part of the pressure tensor $\mathbf{p}$, being calculated from its tensorial virial expression and accessible as time average from the calculated bead trajectories [1]. Each set of measured quantities for a given set of parameters N, γ was simulated (i) by starting up the steady flow with shear rate $\gamma > 0$ from equilibrated samples ($\gamma = 0$) and (ii) by reducing the shear rate from a highly aligned initial conformation, respectively. Within the available precision no discrepancies between the two approaches were found, which only differ (for a given shear rate and chain length) in the time required to reach the stationary state. To check the dependence of the results on the chain length, the samples were depolymerized by cutting the chains during the simulation. Within errors all the measured quantities relax as desired.

The simulation of long chain polymers became feasible by using an optimized parallelized NEMD algorithm on a CRAY T3D parallel machine. The simulation time was still in the order of 1 year on all (16 to 64) processors, and was partially performed during the test period of this machine. The needed CPU time per integration time step and per particle was $\approx 3 \times 10^{-7}$ s per bead and integration step when typically 64 processors were used in parallel. Saving computing time was also achieved by using the efficient sample generators presented in [16].

Rheological behavior.—Rheological properties are extracted for various shear rates over eight decades from $\gamma^* = 10^{-8}$ to $\gamma^* = 1$ for $N = 4$–400. For the short chains ($N < 20$) a weak shear dilatancy is detected. With increasing shear rate the trace of the pressure tensor decreases due to the intramolecular bond stretching and in accord with our findings of flow alignment and structure formation as described for shorter chains in [1]. The non-Newtonian viscosity $\eta \equiv -p_{xy}/\gamma$ is shown for different chain lengths and rates in Fig. 1(a). All the simulated samples show shear thinning, and approach a power law curve $\eta \propto \gamma^{-n}$ independent of M with the exponent $n \approx 0.60 \pm 0.10$. From the non-Newtonian viscosity η in Fig. 1(a) the zero rate viscosity η_0 was estimated by using four different extrapolation schemes [1]; see Fig. 1(b). This quantity clearly exhibits a crossover from a Rouse-type regime $\eta_0^* \propto N^1$ to $\eta_0^* \propto N^{\nu \ge 3}$. For the chain lengths studied it is well represented by the expression $\eta_0^* = 0.7\,N(1 + Z^{\nu-1})$ with a number of "rheologically relevant" entanglements per chain $Z \equiv N/N_c$ and exponent $\nu = 3.3 \pm 0.2$. The zero rate first viscometric function $\Psi_1 \propto (p_{xx} - p_{yy})/\gamma^2$ is found to exhibit a crossover at the same critical chain length.

For the characteristic relaxation times τ_N as defined from the onset of shear thinning at shear rate $\gamma = \gamma_N \equiv 1/\tau_N$ we obtain from the NEMD simulations: $\tau_{10}^* = 10^{1.6}$, $\tau_{30}^* = 10^{2.6}$, $\tau_{60}^* = 10^{3.2}$, $\tau_{100}^* = 10^{3.7}$, i.e., $\tau_N \propto N^{\approx 2}$ for short chains, in accordance with the Rouse model predictions. A fit of the data to the expression $\tau_N^* = c_2 N^2 + c_3 N^3$ gives $c_2 = 3.9$ and $c_3 = 5 \times 10^{-3}$. These values also allow one to estimate an upper limit for the characteristic shear rate for longer chains, e.g., $\tau_{400}^* > 10^6$ holds. Recently, Aoyagi and Doi [2] simulated shear rates down to $\gamma^* = 10^{-4.5} \gg \gamma_{400}^*$ for exactly the same model with $N = 400$, and hence didn't reach the regime by which a zero rate viscosity could have been extracted. In studying long chains with $N = 200$–400 we have chosen $\gamma^* = 10^{-7} < \gamma_N^*$ for these chains lengths. The crossover chain length is detected at $N_c = 100 \pm 10$ beads.

Further discussion and conclusions.—The commonly experimentally accessible quantities characterizing a polymer melt at certain temperature are its monomer density ρ, average M, monomer mass m, squared end-to-end distance per monomer $b^2 \equiv \langle R^2/N \rangle$, the critical and entanglement weights, $M_c = mN_c$ and $M_e = mN_e$, respectively, and the Kuhn length b_K. These quantities are related to the bond length $b_0 = b^2/b_K$, the characteristic ratio $C_\infty = b_k/b_0$, and the so-called tube diameter $d_T = b\sqrt{N_e}$. It has been suggested recently [17] that both N_e and N_c can be calculated from ρ, b^2 and a fixed length $p^* \approx 10^{-9}$ m. In order to compare with our simulation result we rewrite this finding in dimensionless form, which is actually possible only for N_e and then states: $N_e \propto \rho p^3$ with a packing length $p \equiv 1/[\rho\langle R^2/M \rangle] = 1/(nb^2)$. This finding can

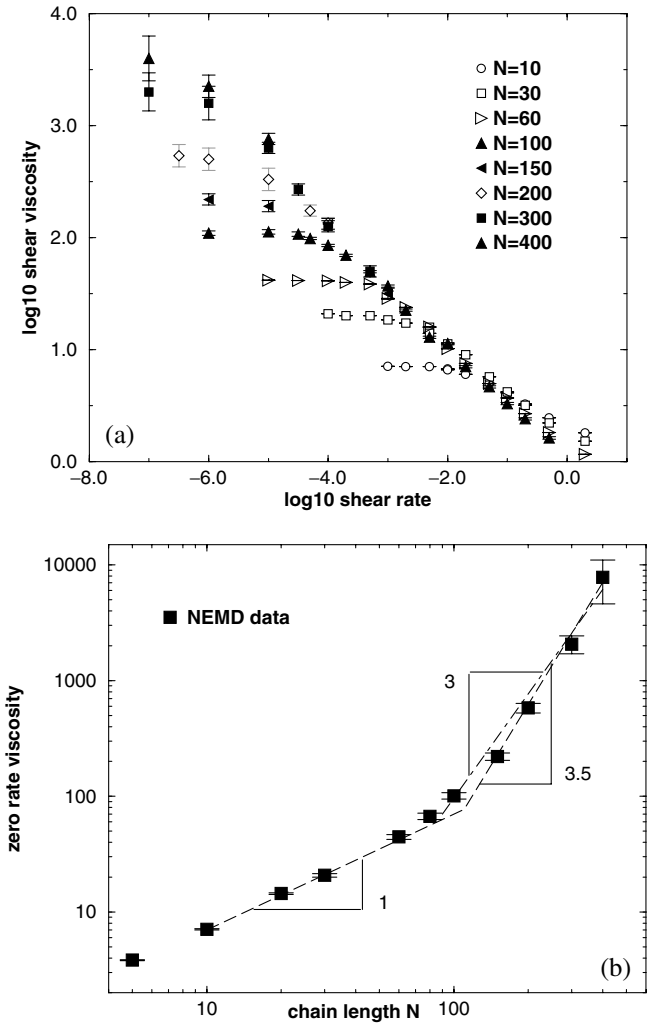

FIG. 1. (a) Non-Newtonian shear viscosity η of the FENE model vs shear rate γ (LJ units) for different chain lengths N. (b) Zero rate shear viscosity η_0 vs chain length.

be also written as (compare the second to the last column of Table I)

$$N_e \propto C_\infty (p/b_K)^2 = [1/(n\, b^3)]^2 , \qquad (1)$$

or $n d_T b^2 = c_e$ with a proportionality coefficient $c_e = 21 \pm 2$. By analyzing experimental data for M_c, we obtained a new relationship (compare the last column of Table I)

$$N_c \propto C_\infty^{3/2} (p/b_K) = 1/(n\, b_0^2\, b) , \qquad (2)$$

in agreement with the simulation data, and a proportionality coefficient of about $c_e^2/5$ such that $C_\infty \sqrt{N_e} \approx 4 N_c$. Thus, we are led to the prediction $N_e n b_0^3 < N_c$ for very flexible chains with $C_\infty < 1.9$. The possibility for the existence of materials with $N_c < N_e$ has been already proposed in [17]. The statement (2) has the advantage upon a different one proposed for N_c in [17], that it exclusively contains dimensionless quantities, and thus allows for a verification by computer simulation. Equations (1) and (2) tell that N_c is inversely proportional to the number of monomers in the volume $b b_0^2$, whereas $\sqrt{N_e}$ is inversely proportional to the number of monomers in the volume b^3.

Under equilibrium conditions the simulated FENE chains exhibit an average bond length $b_0^* = 0.97$, $b = 1.34 b_0$, hence $C_\infty = b^2/b_0^2 = 1.79$ and $p/b_K = 0.404$. Notice that the relationship (1) then predicts a simulation value for $N_e \approx 120$ which is slightly above the one reported for N_c, a factor of 3–4 above the one reported for a dynamical crossover in [9], and just by a factor of 1.5 above the one reported recently from direct measurement of the relaxation modulus [12].

The simulation has to deal with quantities in terms of reference units for mass, length, and energy. These have to be obtained by comparing experiment with simulation and provide the basic length (σ) and energy (ϵ) scale of the LJ potential as well as the mass (m) of a bead in solving Newton's equation. Although some freedom exists in how to adjust three dimensionless units, an accepted one is to obtain the reference energy from the measured temperature $\epsilon_{\rm ref} = T k_B$, the bead mass from the real N_c divided by the simulated one, and σ^2 from the ratio between measured and simulated end-to-end-distances. Sample data such as reported in Table I motivate one to obtain reference units for any simulated quantity for the study of a particular material. For polyethylene (polystyrene), e.g., we deduce a reference length $\sigma = 5.3(9.7)$ Å, a reference mass $m = 42.3(364)$ g/mol, and a reference energy $\epsilon/k_B = 443(490)$ K. From m, σ, ϵ

TABLE I. Contains representative experimental data and the simulation data (FENE model) in dimensionless form. All experimental quantities listed are obtained from literature; data for (i) the ratio between squared end-to-end distance and M, (ii) the mass of a repeating unit, (iii) the critical (from shear flow) and entanglement weights (from plateau modulus), and (iv) bond length b_0 (or C_∞) at temperature T and monomer density ρ (in g/cm^3) of measurement. The last three columns contain universal numbers, if the proposed scaling is valid.

Polymer	T	ρ	b_0	d_T	C_∞	$\frac{N_c}{100}$	$pn^{1/3}$	p/b_K	$\frac{\sqrt{N_e}}{N_c C_\infty}$	$\frac{N_e}{C_\infty}(\frac{b_K}{p})^2$	$\frac{N_c}{C_\infty^{3/2}}(\frac{b_K}{p})$
PE	443 K	0.78	1.45 Å	40.0 Å	7.6	3.0	0.60	0.17	0.25	453	84
PS	490 K	0.92	1.51 Å	88.6 Å	9.9	7.0	0.92	0.29	0.26	454	81
PαMS	459 K	1.04	1.5.7 Å	76.7 Å	10.5	6.9	0.80	0.22	0.27	451	85
PIB	490 K	0.82	1.62 Å	73.4 Å	5.8	6.1	0.97	0.40	0.18	384	109
PDMS	2.98 K	0.97	1.70 Å	74.6 Å	6.0	6.6	0.92	0.36	0.17	417	119
FENE	ε/k_B	$0.84\frac{m}{\sigma^3}$	0.97σ	$1.3\sigma\sqrt{N_e}$	1.79	1	0.66	0.40	$0.018\sqrt{N_e}$	$3.4 N_e$	103

one immediately obtains reference values for any other quantity such as viscosity, time, stress, etc., by dimension analysis: $\sqrt{m\epsilon}/\sigma^2 = 0.07(0.07)$ mPa s, $\sigma\sqrt{m/\epsilon} = 1.8(9) \times 10^{-12}$ s, 40(7.5) MPa, 0.46(0.67) g/cm^3, 553 (109) GHz. Corresponding reference values for other polymers are obtained along this procedure. Care has to be taken when predicting quantities which are sensitive to the ratio between the systems longest and shortest relaxation time (τ_{N_c}/τ_1) such as the shear viscosity (proportional) and the shear rate at the onset of shear thinning (inversely proportional). To illustrate this, for polystyrene the simulation predicts the correct zero shear viscosity $\eta_0 = \sqrt{m\epsilon}/\sigma^2\Gamma\,\eta_0^* = 68$ Pa s (at $N = N_c$) for a factor $\Gamma = 10^4$ which happens to be equal to the ratio of relaxation times $\tau_{N_c}^*/\tau_1^* = 10^4$. Accordingly, from the onset of shear thinning at shear rate $\gamma^* = 10^{-4}$ obtained for the FENE model at $N = N_c$ (see Fig. 1) we predict for the real shear rate (for polystyrene) $\gamma_c = \gamma^*(\sigma/\Gamma)^{-1}\sqrt{\epsilon/m} = 1100\ \mathrm{s}^{-1}$ which is again in agreement with experimental findings [11]. As a result, the shear stress at onset of shear thinning is correctly reproduced without adjustment by Γ, i.e., $(\eta_c\gamma_c)/(\eta_c^*\gamma_c^*) = 7.5$ MPa for polystyrene.

Besides the investigation of rheological behaviors the simulation of bead trajectories allows us to analyze the degree of flow-induced orientation of chain segments. For example, a nonvanishing alignment of chain *ends* is observed in accordance with earlier simulation results for $N \leq 400$ [2] and $N = 32$ [13]. The effect of such an alignment on viscous properties had been worked out [13,18] and compared to data obtained in flow birefringence and small angle neutron scattering experiments. A discussion about structural properties is beyond the scope of this paper.

In order to correlate the rheological behavior with the degree of entanglement one needs a definition of an "entanglement." We probed the definition for an entanglement radius as introduced in [8]. It is based on the mutual overlap of static contour volumes for pairs of chains. Our result from this investigation is that there is no visible crossover in the number of these entanglements or the distribution of entanglements at $N = N_c$. We therefore conclude that in order to keep the idea of localized entanglement, that (i) this definition does not match the intuitive picture about entanglements, that (ii) few entanglements lead to a strong increase in stresses, or that (iii) one has to account for collective effects (correlations in the overlap caused by more than two chains, by keeping the same concept). Since we observed the rheological crossover and also reported the value for N_c, the model should definitely serve to define entanglements based on the information contained in the simulated coarse grained phase space of linear polymers. However, the simple relationships (1) and (2) for N_c, N_e in terms of purely geometrical quantities p/b_K and C_∞ already reflect the "topological" and inherently nonlocal origin of entanglement behavior. Another aspect to be recalled in this context is that in our simulations at low rates and during relaxation, stress contributions from nonbonded interactions dominate in the long time regime (where at the same time the stress-optic rule is valid [3]).

The actual findings underline the relevance of the FENE model in predicting static, dynamic, and flow behaviors of real polymers for arbitrary weights. Forthcoming investigations for long chains far above the critical weight reported here clearly rely on the availability of the necessary computing power and an ongoing improvement of algorithmic methods.

This work was financially supported by the Sfb 605 "Elementarreibereignisse" (DFG) and the Minerva foundation, Germany. We thank the ZIB Berlin and the ETH Zürich for providing us with their supercomputing facilities.

[1] M. Kröger, W. Loose, and S. Hess, J. Rheol. **37**, 1057 (1993).
[2] T. Aoyagi and M. Doi, Comput. Theor. Polym. Sci. **10**, 317 (2000).
[3] J. Gao and J. H. Weiner, J. Chem. Phys. **90**, 6749 (1989); M. Kröger, C. Luap, and R. Muller, Macromolecules **30**, 526 (1997).
[4] T. P. Lodge, N. A. Rotstein, and S. Prager, Adv. Chem. Phys. **79**, 1 (1990).
[5] J. Klein, Nature (London) **271**, 143 (1978); P. Schleger, B. Farago, C. Lartigue, A. Kollmar, and D. Richter, Phys. Rev. Lett. **81**, 124 (1998).
[6] R. F. Landel, J. W. Berge, and J. D. Ferry, J. Colloid. Sci. **12**, 400 (1957); H. H. Meyer, W. J. Pfeiffer, Jr., and J. D. Ferry, Biopolymers **5**, 123 (1967).
[7] T. A. Witten, Rev. Mod. Phys. **71**, S367 (1999); H. Voigt, *Struktur und Dynamik von Kettenverschlaufungen in Polymersystemen* (W&T Publishing, Berlin, 1996); R. Y. Qian, J. Macromol. Sci. Phys. B **38**, 75 (1999); A. L. Kholodenko and T. A. Vilgis, Phys. Rep. **298**, 254 (1998); J. Rault, J. Non-Newt. Fluid. Mech. **23**, 229 (1987).
[8] M. Kröger and H. Voigt, Macromol. Theory Simul. **3**, 639 (1994).
[9] K. Kremer, G. S. Grest, and I. Carmesin, Phys. Rev. Lett. **61**, 566 (1988); K. Kremer and G. S. Grest, J. Phys. Chem. **92**, 5057 (1990).
[10] J. Gao and J. H. Weiner, J. Chem. Phys. **103**, 1621 (1995).
[11] J. D. Ferry, *Viscoelastic Properties of Polymers* (J. Wiley & Sons, New York, 1980).
[12] M. Pütz, K. Kremer, and G. S. Grest, Europhys. Lett. **49**, 735 (2000).
[13] M. Kröger and S. Hess, Physica (Amsterdam) **195A**, 336 (1993); M. Kröger, Physica (Amsterdam) **249A**, 332 (1998).
[14] M. Doi and S. F. Edwards, J. Chem. Soc. Faraday Trans. II **74**, 1789 (1978); **74**, 1818 (1978); **75**, 38 (1979).
[15] G. S. Grest, B. Dünweg, and K. Kremer, Comput. Phys. Commun. **55**, 269 (1989).
[16] M. Kröger, Comput. Phys. Commun. **118**, 278 (1999).
[17] L. J. Fetters, D. J. Lohse, S. T. Milner, and W. W. Graessley, Macromol. **32**, 6847 (1999).
[18] D. W. Mead, R. G. Larson, and M. Doi, Macromolecules **31**, 7895 (1998).